

Attention Hijackers: Detect and Disentangle Attention Hijacking in LVLMs for Hallucination Mitigation

Beitao Chen¹

chenbeitao@gmail.com

Xinyu Lyu^{2,4}

xinyulyu68@gmail.com

Lianli Gao¹

lianli.gao@uestc.edu.cn

Jingkuan Song^{1,3}

jingkuan.song@gmail.com

Heng Tao Shen^{1,3}

shenhengtao@hotmail.com

¹Center for Future Media, University of Electronic Science and Technology of China

²Southwestern University of Finance and Economics, Chengdu, China

³Tongji University

⁴Engineering Research Center of Intelligent Finance, Ministry of Education

Abstract

Despite their success, Large Vision-Language Models (LVLMs) remain vulnerable to hallucinations. While existing studies attribute the cause of hallucinations to insufficient visual attention to image tokens, our findings indicate that hallucinations also arise from interference from instruction tokens during decoding. Intuitively, certain instruction tokens continuously distort LVLMs' visual perception during decoding, hijacking their visual attention toward less discriminative visual regions. This distortion prevents them integrating broader contextual information from images, ultimately leading to hallucinations. We term this phenomenon “**Attention Hijacking**”, where disruptive instruction tokens act as “**Attention Hijackers**”. To address this, we propose a novel, training-free strategy namely **Attention HIjackers Detection and Disentanglement (AID)**, designed to isolate the influence of Hijackers, enabling LVLMs to rely on their context-aware intrinsic attention map. Specifically, AID consists of three components: First, **Attention Hijackers Detection** identifies Attention Hijackers by calculating instruction-driven visual salience. Next, **Attention Disentanglement mechanism** is proposed to mask the visual attention of these identified Hijackers, and thereby mitigate their disruptive influence on subsequent tokens. Finally, **Re-Disentanglement** recalculates the balance between instruction-driven and image-driven visual salience to avoid over-masking effects. Extensive experiments demonstrate that AID significantly reduces hallucination across various LVLMs on several benchmarks. Project page: <https://github.com/BT-C/AID>.

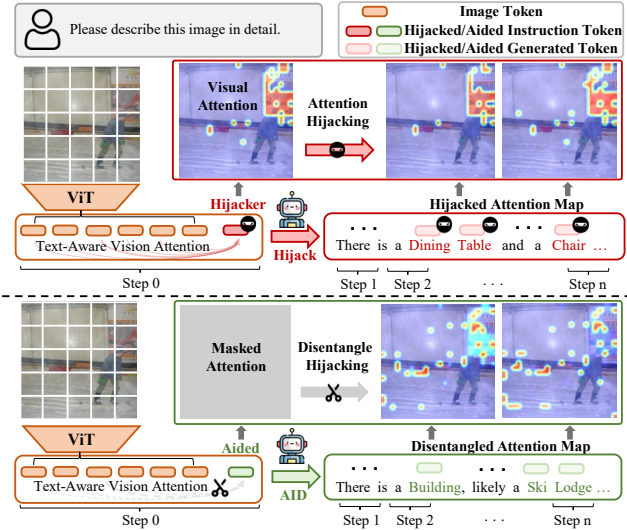


Figure 1. **Upper part:** shows Attention Hijacking, where the Hijacker’s erroneous attention map disrupts generated tokens, causing hallucinations. **Lower part:** illustrates how our proposed AID isolates Hijacker’s influence, allowing the LVLML to rely on its context-aware attention map, thus reducing hallucinations.

1. Introduction

Large Vision-Language Models (LVLMs) have recently demonstrated remarkable advancements, showcasing impressive performance across a wide range of tasks. [1, 5, 11, 14, 25, 36, 43, 55]. Despite their remarkable versatility, LVLMs encounter a significant challenge known as hallucination. Specifically, this issue arises when there is a discrepancy between the textual output generated by the model and the actual visual input [18, 27, 30, 35]. Such mismatches may

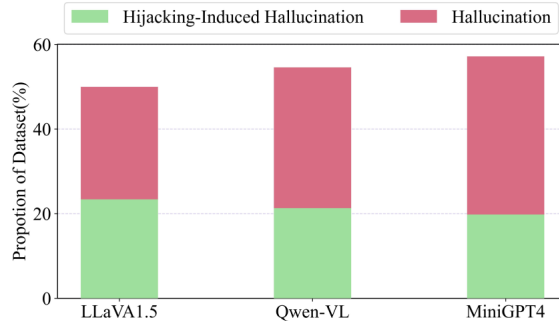


Figure 2. **The proportion of Hijacking-Induced hallucinations** across different LVLMs.

manifest as irrelevant or nonsensical responses, or in inaccuracies regarding colors, quantities, and locations of objects that do not appear in the image.

Existing research can be categorized into two types. The first relies on supervised fine-tuning [7, 30, 41, 48, 53], which requires the creation of high-quality datasets, involving significant training costs. To make hallucination mitigation training-free, recent works [3, 17, 20, 33, 46] have explored attention mechanisms and proposed inference-based methods to reduce hallucinations. While existing studies attempts to make models more interactive with image tokens, they overlook the visual influence of instruction tokens during LVLMs’ decoding process. This oversight limits the effectiveness of these methods in hallucination mitigation.

Our observations show that visual information conveyed by instruction tokens can significantly distort LVLMs’ visual perception when generating subsequent tokens, accounting for up to 46.7% of total hallucinations (Fig. 2). Specifically, the instruction token prompts the LVLMs to repeatedly attend to the same image area with similar attention maps (Fig. 1). The underlying reason is that the attention distribution of LLM decoder on image tokens closely mirrors that of the visual encoder (i.e., ViT [13]), with both distributions concentrating on background elements rather than the intended objects in the image (Fig. 4). This misdirection causes the model to persistently focus on these misleading regions during subsequent auto-regressive processes, ignoring the broader contextual area and ultimately leading to hallucinations. As illustrated in Fig. 1, Attention Hijacker makes model continuously focus on negative local regions around the *poster* while ignoring the surrounding context of the *building* and the *skier* during decoding process, resulting in hallucinations such as *dining table* and *chair*. We term this pattern as **Attention Hijacking**, and we refer to the instruction tokens responsible for this pattern as **Attention Hijackers**.

The above challenges motivate us to study two problems: (1) how to identify Attention Hijackers among instruction

tokens, and (2) how to efficiently isolate the influence of identified hijackers, allowing the model to independently explore appropriate visual interaction patterns. Inspired by [37], our key intuition is that LVLMs’ internal visual attention reflect the likelihood of hallucinations, which can be mitigated by modifying the attention weights of these hijacker tokens during the decoding process. Accordingly, we identify Attention Hijackers by assessing the volume of visual information that instruction tokens impose on subsequently generated tokens via visual attention map. The rationale is that the more visual information an instruction token contributes, the more likely generated token’s visual attention may get hijacked by it. Once hijackers are identified, their disruptive influence on less discriminative visual regions can be isolated, restoring the model’s context-aware attention capability.

Based on the above analysis, we propose a novel, training-free strategy, **Attention Hijackers Detection and Disentanglement**, which isolates the influence of Hijackers, allowing LVLMs to utilize their context-aware intrinsic attention map. Specifically, the process begins with **Attention Hijackers Detection**, which identifies Attention Hijackers by calculating instruction-driven visual salience. Next, **Attention Disentanglement** mechanism is introduced to mask the visual attention of the previously identified hijackers. Finally, to prevent excessive masking of the visual perception of non-hijacker instruction tokens made by Attention Disentanglement, **Re-Disentanglement** is proposed to adjust the balance between instruction-driven and image-driven visual salience, ensuring effective disentanglement.

In conclusion, our main contributions are summarized as follows:

1. We, for the first time, identify that hallucinations stem from the disruptive interactions with certain instruction tokens (i.e., Attention Hijacker) and conduct an in-depth analysis of how these hijackers interfere model’s visual attention, elucidating the mechanisms by which this disruption leads to hallucinations.
2. Based on our exploration, we propose **Attention Hijackers Detection and Disentanglement (AID)**, a training-free strategy that first locates potential Attention Hijackers and disentangles hijacked attention from the Attention Hijacker by cutting-off the visual source associated with the Attention Hijacker.
3. Through comprehensive experiments, we demonstrate our proposed AID achieves significant improvements in alleviating hallucinations without requiring additional training or the use of external tools.

2. Related Work

Hallucination in LVLMs. In Vision-Language Models (VLMs), “object hallucination”—where models generate plausible but mismatched or missing objects in images—is a known issue [6, 27, 39]. Traditional VLMs address this

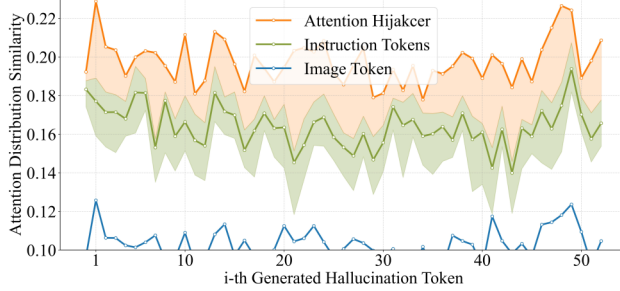


Figure 3. Illustration of Attention Hijacking. The Attention Hijacker (orange curve) shows a visual attention distribution more aligned with the hallucination token than with the image token (blue curve), indicated by consistently higher similarity values.

through fine-grained contrastive learning [51], ROI feature fusion [6], and data augmentation to reduce co-occurrence patterns [23]. However, these techniques to autoregressive LVLMs is challenging [22, 44]. Recent research on LVLMs focuses on developing evaluation and detection methods [27, 29, 35, 42] for hallucination, such as the CHAIR metric[39] for caption accuracy and POPE[27] for binary object recognition. Further progress includes creating refined datasets for fine-tuning [18, 26, 29], training post-hoc revisors [54], and using factually augmented Reinforcement Learning from Human Feedback (RLHF) [41].

Attention Deficits of LVLMs. A key approach to reduce hallucinations in LVLMs is to address attention deficits by adjusting or decoding strategies [3, 17, 20, 33, 46]. Early studies [12, 17] showed that LVLMs often focus on global image features, neglecting prompt-relevant details [3], a limitation linked to the Vision Transformer encoder [2]. To counter this, some methods adaptively amplify attention weights for relevant image tokens [33], while others filter effective image information based on attention scores, reducing hallucinations via contrastive decoding [20]. Recent advances, like Concentric Causal Attention, further mitigate object hallucinations by addressing long-term decay in Rotary Position Encoding [46].

Existing methods attempt to mitigate hallucinations by adjusting LVLMs’ attention to relevant visual elements, yet they often overlook disruptions caused by specific instruction tokens. Our approach isolates disruptive influences, restoring accurate attention and significantly reducing hallucinations across benchmarks.

3. Method

3.1. Problem Formulation

Autoregressive language decoders. Each attention head in a single layer performs repeated attention operations with

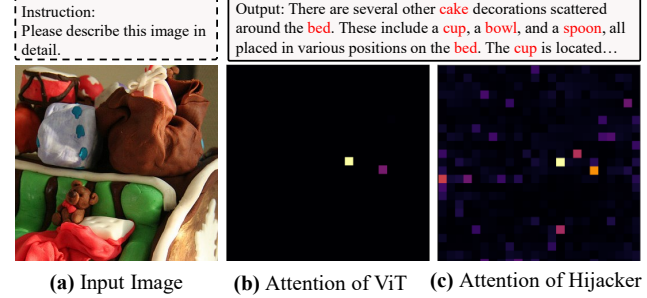


Figure 4. Attention deficiencies of Visual Encoder (ViT). Vision Transformer overemphasizes background regions with high-norm outlier tokens, resulting in hallucinations through Attention Hijacking.

identical input shapes:

$$O_h = A_h V_h, \quad A_h = \text{softmax} \left(\frac{Q_h K_h^\top}{\sqrt{d_k}} \right). \quad (1)$$

Each attention head h uses its own set of queries $Q_h \in \mathbb{R}^{n \times d_k}$, keys $K_h \in \mathbb{R}^{n \times d_k}$, and values $V_h \in \mathbb{R}^{n \times d_k}$, where n is the sequence length and d_k represents hidden dimensions. The output $O_h \in \mathbb{R}^{n \times d_k}$ is calculated by multiplying V_h with attention weights $A_h \in \mathbb{R}^{n \times n}$, with each row representing the weights for each token during feature mixing.

3.2. Analysis of Attention Hijacking

Observations of Attention Hijacking. (i) To examine how attention hijacking occurs, we measured the similarity in visual attention between certain instruction tokens and hallucinated tokens, as shown in Fig. 3. The results reveal that hallucinated tokens get persistently interfered by the Attention Hijacker (orange curve), maintaining a high Attention Distribution Similarity scores across all hallucination tokens. (ii) Furthermore, we observed that Attention Hijacker (orange curve) exhibits a higher Attention Distribution Similarity than the image token (blue curve), suggesting that generated tokens are more affected by certain instruction tokens (i.e., Attention Hijackers) than by actual image content. (iii) Lastly, we observed that different instruction tokens exert varying degrees of influence on the model, as indicated by different levels of Attention Distribution Similarity (green v.s., orange) in Fig. 3. This motivates us to develop a hijacker detection mechanism to identify tokens with the strongest interference during decoding process, as elaborated in Sec. 3.3.

Mechanism of Attention Hijacking’s Sustainable Impact. In autoregressive process, generated tokens are influenced by preceding instruction tokens, with this impact reinforced by the KV-cache [38], which retains and reuses past attention patterns. Certain instruction tokens, or “Attention Hijackers,” impose strong, localized attention that persists through the KV-cache, causing subsequent tokens to focus on irrelevant

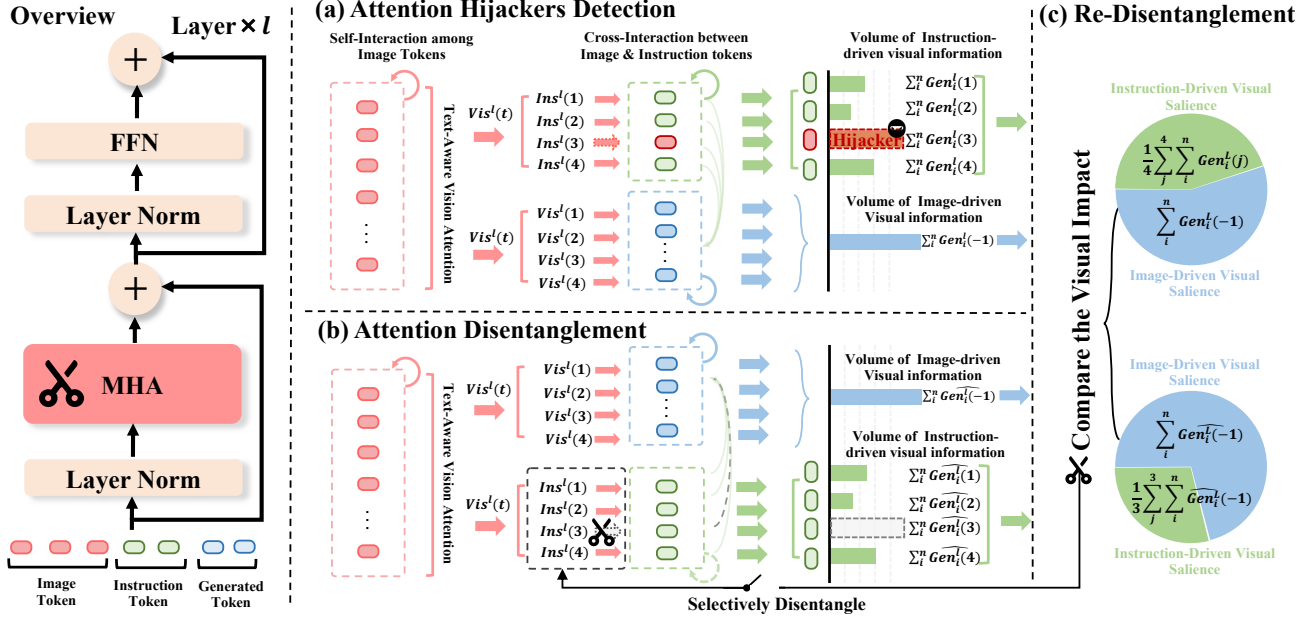


Figure 5. **The framework of our AID.** The proposed framework consists of three key components: Attention Hijackers Detection, which identifies hijackers by calculating instruction-driven visual salience; Attention Disentanglement, which masks the visual attention of identified hijackers to isolates the influence of Hijackers; and Re-Disentanglement, which adjusts the balance between instruction-driven and image-driven salience to prevent over-masking and ensure effective Disentanglement.

visual cues rather than adapting to broader image contexts. This KV-cache persistence amplifies hijacker influence, directing attention toward misleading regions.

Why Attention Hijacking Leads to Hallucinations? We hypothesize that the Vision Transformer (ViT) overemphasizes background regions with high-norm outlier tokens, resulting in hallucinations through Attention Hijacking. This misdirects the model's focus to irrelevant areas, causing it to overlook essential details and misinterpret the visual context. To verify this hypothesis, we visualize the visual attention of the Vision Transformer (ViT) and that of the Attention Hijacker in Fig. 4. Fig. 4 (b) illustrates the influence of high-norm outlier tokens on ViT's visual attention, which typically correspond to background areas associated with negative visual priors [12]. Meanwhile, the attention of the instruction token depicted in Fig. 4 (c) exhibits a distribution similar to ViT's in Fig. 4 (b). This similarity may arise because, when these image tokens are projected into the LLM, their high attention values in the visual encoder lead the model to disproportionately focus on them, resulting in the neglect of local details in other patches. This finding aligns with the conclusion elaborated in [17].

Solution. The limitations of Vision Transformers (ViT) can be addressed by continuously increasing the visual perception and fine-grained understanding of the model. However, the generation of fine-grained annotated data and the training of visual encoders are both prohibitively expensive [8].

Inspired by [52], our core insight is that LVLMs' internal visual attention reflects the likelihood of hallucinations, which can be reduced by adjusting the attention weights of hijacker tokens during decoding. To achieve this, we propose Attention Hijackers Detection and Disentanglement (AID) (shown in Fig. 5) to firstly identify Attention Hijackers by analyzing the visual influence that instruction tokens impose on subsequent tokens through attention analysis. Then, by adaptively masking the attention maps of these hijackers, we redirect the model's focus from less informative visual regions to broader contextual areas in the image. The process for identifying Attention Hijackers and restoring the model's context-aware visual attention are discussed in the following sections.

3.3. Attention Hijackers Detection

Based on findings from Sect. 3.2, we propose the Attention Hijackers Detection method to detect Attention Hijackers by calculating the volume of instruction-driven visual information across all tokens, as shown in Fig. 5 (b). This process involves two integration phases, i.e., Self-Interaction of Image Tokens and Cross-Interaction between Image & Instruction tokens, followed by a attention-based information aggregation phase, i.e., Visual Information Transmission to Generated Tokens.

Self-Interaction among Image Tokens. The self-interaction of image tokens redistributes model's visual atten-

tion, making later tokens carry more than earlier ones (Fig. 7) and providing varying levels of visual information to the hijacker. Therefore, prioritizing these calculations is essential. The self-interaction among image tokens is calculated as follows:

$$Vis^l(t) = \begin{cases} 1, & l = 0 \\ \sum_{j \in \mathbb{I}_{(t, vis)}^l} (1 + w_j) Vis^{l-1}(j), & l > 0 \end{cases}, \quad (2)$$

where $Vis^l(t)$ represents visual information of t th image token on l th layer, $\mathbb{I}_{(t, vis)}^l$ indicates index of visual attention weight associated with the t th image token's self-interaction and w_j is the j th visual attention weight. We initialize visual information in 0 th layer to be identical across all image tokens, allowing it to evolve through subsequent interactions.

Cross-Interaction between Image & Instruction tokens. In this step, the visual information get integrated into the instruction tokens, either directly from the image or indirectly from the previous instruction tokens. The calculations are shown below:

$$Ins^l(t) = \begin{cases} 0, & l = 0 \\ \sum_{j \in \mathbb{I}_{(t, ins)}^l} w_j Vis^{l-1}(j) \\ + \sum_{j \in \mathbb{I}_{(t, ins)}^l} (1 + w_j) Ins^{l-1}(j), & l > 0 \end{cases}, \quad (3)$$

where $Ins^l(t)$ denotes the visual information of t -th instruction token on l -th layer, with $\mathbb{I}_{(t, ins)}^l$ indicating the index of visual attention weight associated with the t -th instruction token and w_j as the j -th visual attention weight. In 0 th layer, visual information of all instruction tokens is initialized to zero, as these tokens originate from user prompts and lack visual modality data. In subsequent layers, each instruction token integrates visual information both directly from image tokens and indirectly from previous-layer instruction tokens that have absorbed visual information.

Visual Information Transmission to Generated Tokens. This step measures the volume of visual information from each instruction token to generated tokens, which primarily derives from three components: (1) the instruction token, and (2) the tokens generated in previous step. The calculations are shown below:

$$Gen_i^l(t) = \begin{cases} w_t Ins^l(t) \\ + \sum_{j \in \mathbb{I}_{(t, Gen)}^l} w_j Gen_j^l(t), & l = 0, t \neq -1 \\ w_t Ins^l(t) + (1 + w_i) Gen_i^{l-1}(t) \\ + \sum_{j \in \mathbb{I}_{(t, Gen)}^l} w_j Gen_j^l(t), & l > 0, t \neq -1 \end{cases}, \quad (4)$$

where $Gen_i^l(t)$ denotes the visual information contributed by the t -th instruction token to the i -th generated token. $\mathbb{I}_{(i, vis)}^l$ represents the index of visual attention weight associated with the i -th generated token. Finally, find $\mathbb{S}_H = \{t_1, t_2, \dots, t_k\}$ such that $|\mathbb{S}_H| = k$ and $\forall x \in \mathbb{S}_H, \forall y \notin \mathbb{S}_H$,

where \mathbb{S}_H is the **Attention Hijackers**.

$$\sum_{i \in \mathbb{I}_{gen}} Gen_i(x) > \sum_{i \in \mathbb{I}_{gen}} Gen_i(y). \quad (5)$$

3.4. Attention Disentanglement

After identifying Attention Hijackers in Sect. 3.3, we implement the Attention Disentanglement mechanism to disentangle model's visual attention from hijacker tokens. This method selectively blocks hijackers from receiving visual information while preserving relevant visual cues for non-hijacking tokens. Thereby, it refocuses the model on accurate visual regions, reducing hallucinations and enhancing the alignment with intended visual content.

Specifically, we disconnect all visual information received by the hijacker during the visual-textual interaction, as shown in Fig. 5(b). Practically, we cut-off all tokens carrying image information (including image tokens and non-hijacking instruction tokens with visual information) from interacting with the hijacker, while ensuring that non-hijacking instruction tokens still receive image information as specified in Eqn. 3. The specific cut-off operation is shown in the following formula:

$$DIns^l(t) = \begin{cases} Ins^0(t), & l = 0 \\ \sum_{j \in \mathbb{I}_{(t, ins)}^l} (1 + w_j) DIns^{l-1}(j), & l \leq l_k \end{cases}, \quad (6)$$

where $DIns^l(t)$ represents the intermediate instruction token generated after Attention Disentanglement, containing only results related to the hijacker, as shown in:

$$Ins^l(t) = DIns^l(t), t \in \mathbb{S}_H. \quad (7)$$

For other non-hijacking instruction tokens, the standard interactions defined in Eqn. 3 are retained.

3.5. Re-Disentanglement

The methods in Sect. 3.4 risk disrupting valuable visual interactions by broadly masking instruction tokens, which may unintentionally diminish the contributions of non-hijacking instruction tokens, especially when they provide essential contextual information for comprehensive visual understanding.

To address this, we propose the Re-Disentanglement mechanism to selectively disengages the Hijacker's influence by comparing the instruction-driven and image-driven visual salience, as shown in Fig. 5 (c). Specifically, it compares the visual impact (i.e., instruction-driven visual salience) of each instruction token with that of the image token (i.e., image-driven visual salience), disengaging attention only when the instruction token's impact decreases relative to the image token. A decrease in impact indicates that the instruction token no longer contributes relevant visual context. If no decrease is detected, it suggests that the instruction token is still

Methods	LLaVA-1.5			MiniGPT-4			mPLUG-Owl2		
	Random	Popular	Adversarial	Random	Popular	Adversarial	Random	Popular	Adversarial
Greedy	81.75	78.48	76.54	69.96	66.77	67.93	82.20	80.49	78.54
Beam Search	84.84	83.87	81.61	69.64	67.01	68.30	86.83	83.92	81.73
OPERA	82.03	81.49	79.74	69.62	67.23	68.29	87.29	82.53	80.25
VCD	80.42	76.05	75.95	68.82	66.80	66.26	80.50	78.51	78.67
DoLa	83.56	83.37	80.97	69.85	67.70	68.65	88.11	84.75	82.17
Ours	90.12	88.77	85.57	75.41	70.01	70.29	90.81	86.72	84.52

Table 1. Comparison of the average F1-score evaluation results under different settings (i.e., *Random*, *Popular*, *Adversarial*) using various baselines and our AID on offline POPE benchmark [9, 27] over five random runs, where higher F1-score indicates better performance. † denote results reproduced with the authors’ codes. More detailed statistical results are shown in Tab.1 of Appendix A.

Methods	LLaVA-1.5			MiniGPT-4			mPLUG-Owl2		
	CHAIR _s ↓	CHAIR _i ↓	Recall↑	CHAIR _s ↓	CHAIR _i ↓	Recall↑	CHAIR _s ↓	CHAIR _i ↓	Recall↑
Greedy	48.0	14.7	76.9	39.2	15.6	56.8	55.0	17.8	72.0
Beam Search	50.0	15.5	77.8	40.2	16.1	57.3	59.0	17.8	72.8
OPERA	47.3	14.8	76.8	41.4	15.0	58.0	56.3	18.1	71.2
VCD	50.4	15.7	76.4	39.6	16.2	55.5	62.8	19.8	70.7
DoLa	48.6	14.6	77.5	40.0	16.3	57.5	54.8	17.4	72.7
Ours	41.8	13.0	77.1	34.0	11.0	55.1	53.0	17.1	71.5

Table 2. Comparison of the average CHAIR evaluation results (instance levels CHAIR_i and sentence levels CHAIR_s) and Recall during decoding with different baselines on MSCOCO datasets of five random runs. Experimental results on more backbones (including GLM-4V and Qwen-VL) are shown in Tab.2 of Appendix A.

aligned with the image information, and its visual influence is preserved. This approach ensures that only instruction tokens introducing misdirecting attention are modified, while those providing meaningful visual guidance remain effective in directing the model’s focus.

Piratically, we first extend Eqn. 4 to compute the visual information contributed by the image token to the generated token:

$$Gen_i^l(t) = \begin{cases} \sum_{j \in I_{i,vis}} w_j Vis^l(j), & l = 0, t = -1 \\ \sum_{j \in I_{i,vis}} w_j Vis^l(j) \\ +(1 + w_i) Gen_i^{l-1}(t), & l > 0, t = -1 \end{cases} \quad (8)$$

where $Gen_i^l(-1)$ represent the visual information directly from image token.

Then, the difference between instruction-driven and image-driven visual salience are formulated as follows:

$$\sum_{i \in I_{gen}} \left(\sum_{t \in I_{ins}} \frac{Gen_i^L(t)}{Gen_i^L(-1)} \right) - \sum_{i \in I_{gen}} \left(\sum_{t \in I_{ins}} \frac{\hat{Gen}_i^L(t)}{\hat{Gen}_i^L(-1)} \right) > 0, \quad (9)$$

where \hat{Gen}_i^L denotes the visual information contributed by the t -th instruction token to the i -th generated token. And, the Hijacker’s visual influence is removed once the conditions specified in Eqn.9 are satisfied.

4. Experiments

4.1. Experiment Setup

Benchmarks. Following common settings [9, 27], We evaluate the effectiveness of our AID in VH mitigation across five widely used benchmarks: (1) the offline Polling-based Object Probing Evaluation (POPE) [9, 27] on the MSCOCO dataset; (2) the CHAIR [39] quantitative metrics on MSCOCO dataset [28]; (3) three general-purpose benchmarks: LVLM Comprehensive Evaluation (MME) [15], Multimodal Benchmark (MMBench) [34], and Multimodal Veterinarian (MM-Vet) [50].

Baselines. We compare our AID with greedy decoding, beam search decoding, and several state-of-the-art (SOTA) decoding methods as baselines, including DoLa [10], OPERA [19], and VCD [24]. All these methods adopt the beam search decoding strategy with a beam size of 3.

Backbones. Following previous studies [9, 27], we select five widely used LVLMs families, e.g., LLaVA-1.5 [32], MiniGPT-4 [56], mPLUG-Owl2 [47], GLM-4V [16] and Qwen-VL-Chat [4], as the base models for all baselines. We analyze the VH of these LVLMs under different decoding to evaluate the effectiveness of our AID.

Settings. Following HALC [9], we implement the proposed AID using Hugging Face Transformers library [45] and employ beam search for decoding. The LLaVA1.5-7B re-

Methods	LLaVA-1.5				MiniGPT-4				mPLUG-Owl2			
	Object-level↑		Attribute-level↑		Object-level↑		Attribute-level↑		Object-level↑		Attribute-level↑	
	Existence	Count	Position	Color	Existence	Count	Position	Color	Existence	Count	Position	Color
Greedy	165.67	120.00	110.67	148.33	137.00	93.00	75.00	125.00	167.00	120.00	105.00	145.00
DoLa	170.00	120.00	106.67	150.67	137.00	90.00	75.33	122.67	167.00	125.00	110.00	147.67
OPERA	165.00	115.67	104.00	145.00	140.67	92.33	73.00	125.00	167.00	122.33	100.00	145.00
VCD	175.33	130.33	115.00	155.00	142.00	95.33	71.33	129.00	171.33	125.00	107.33	150.00
HALC	167.67	121.33	106.67	150.67	140.00	92.67	71.33	122.67	167.00	120.33	108.67	145.00
VASparse	180.00	132.67	121.33	160.00	147.33	98.67	78.67	133.00	175.00	130.00	110.67	155.00
Ours	195.00	150.00	130.00	170.00	170.00	96.66	93.33	133.33	180.00	143.33	106.66	155.00

Table 3. Results on the subset of the MME benchmark for evaluating object-level and attribute-level VH, where the best performances within each setting are bolded. We randomly run it five times to obtain the average result, with the whole statistical results in Appendix.

Method	gn_kw_rec	rec	ocr_sp	ocr	ocr_sp_rec	ocr_kw_rec	ocr_gn_sp	Total
LLaVA1.5-7B	18.1 $\uparrow 0.0$	67.6 $\uparrow 0.0$	17.7 $\uparrow 0.0$	48.3 $\uparrow 0.0$	60.0 $\uparrow 0.0$	21.2 $\uparrow 0.0$	10.0 $\uparrow 0.0$	31.1 $\uparrow 0.0$
+ VCD	19.2 $\uparrow 1.1$	62.2 $\downarrow 5.4$	15.8 $\downarrow 1.9$	29.2 $\downarrow 20.0$	42.5 $\downarrow 17.5$	17.5 $\downarrow 3.7$	60.0 $\uparrow 50.0$	30.2 $\downarrow 1.1$
+ OPERA	21.8 $\uparrow 3.7$	61.9 $\downarrow 5.7$	21.5 $\uparrow 3.8$	51.7 $\uparrow 3.4$	56.2 $\downarrow 3.8$	11.2 $\downarrow 10.0$	30.0 $\uparrow 1.4$	32.0 $\uparrow 0.9$
+ Ours	19.5 $\uparrow 1.4$	70.3 $\uparrow 2.7$	18.5 $\uparrow 0.8$	55.0 $\uparrow 6.7$	58.3 $\downarrow 1.7$	27.8 $\uparrow 6.6$	12.5 $\uparrow 2.5$	31.8 $\uparrow 0.7$

Table 4. **The MM-Vet evaluation** results encompass multiple complex multimodal tasks. *gn* represents language generation, *kw* indicates knowledge, *sp* denotes spatial awareness, and *rec* stands for recognition.

sults are based on version 1.2.2 from the official benchmark repository [31]. The effectiveness of methods such as VCD, DOLA, and OPERA is evaluated using the HALC implementation [9]. We conduct experiments with a maximum generation length L_{max} of 64 for offline POPE and 1024 for CHAIR. The beam size is set to 3, except for $L_{max} = 512$, where it is set to 2. All experiments, including the decoding process of LVLMs, are conducted on eight V100 GPUs. Other methods follow the settings specified in their respective original papers. Further details and results are provided in the Appendix B.

4.2. Main Results

POPE Evaluation. To evaluate AID’s capability on object hallucination, following HALC [9], We employ the offline POPE (OPOPE) benchmark, using the F1-score as the evaluation metric for VH, where offline checks substitute the live interactions of POPE. As shown in Table 1, we have several observations: (1) AID consistently attains superior performance across most settings, surpassing both state-of-the-art methods, further validating its effectiveness; (2) AID effectively mitigates VH across three distinct LVLM architectures, showcasing its versatility and plug-and-play capability.

CHAIR Evaluation. To evaluate our model’s performance in open-ended caption generation with the CHAIR benchmark. Following HALC [9], we set ‘*Please describe this image in detail.*’ as the input prompt, as shown in Table 2. From the results, we derive several detailed observations: (1) It can be observed that our method significantly outperforms

existing methods for reducing VH. (2) Our AID achieved the lowest VH rate at both the sentence and instance levels across three LVLM families while preserving recall, highlighting its superiority and generalizability in mitigating VH.

MME Evaluation. Following [9, 57], we adopt object-level subsets (“existence” and “count”) and attribute-level subsets (“position” and “color”) of MME benchmark [15] to evaluate VH. As shown in Table 3, we can observe that: (1) Our AID can significantly reduce object and attribute hallucination, and achieve optimal VH mitigation performance. (2) DoLA and OPERA do not exhibit significant VH mitigation on the MME benchmark. This is because the MME evaluation is a binary classification task, requiring LVLMs to generate only a few tokens, which constrains methods reliant on longer sequences and special entity handling.

General-Purpose Evaluation. To verify that our AID method does not compromise the model’s generalization capability, we evaluated AID on multiple benchmarks, including MMBench, MM-Vet, and MME. The results from MMBench (Fig. 6) show that AID is highly competitive compared to state-of-the-art (SOTA) methods, with detailed findings provided in Appendix. Notably, as shown in Tab. 4, AID achieves significant overall performance improvements, particularly in OCR and spatial reasoning tasks, with an average increase of 6.7%. Finally, the model demonstrates superior generalization capabilities and enhanced hallucination mitigation when compared to VCD and OPERA method on MME (elaborated in Tab. 3). Full experimental results are available in to Appendix for further reference.

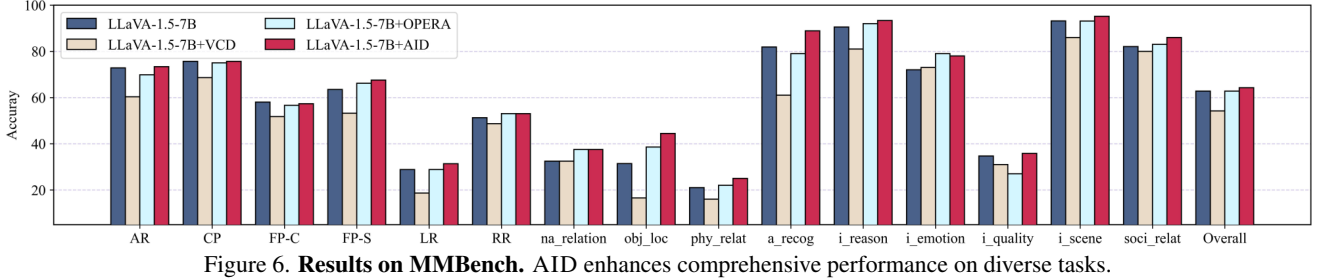


Figure 6. **Results on MMBench.** AID enhances comprehensive performance on diverse tasks.

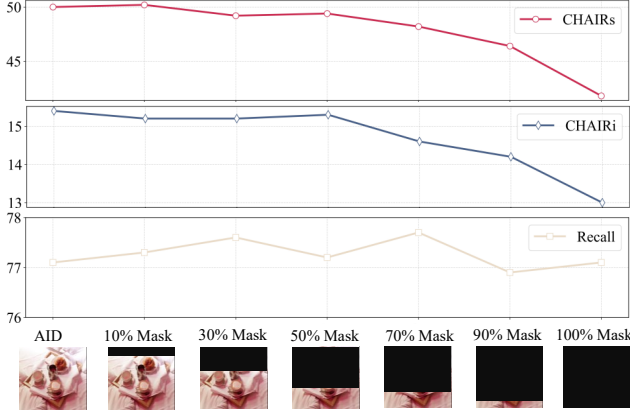


Figure 7. **Ablation Studies** of masking different proportions of visual areas in Attention Hijackers.

Method	CHAIR _s ↓	CHAIR _I ↓	Recall ↑
LLaVA-1.5	50.0 ↑0.0	15.4 ↑0.0	77.1 ↑0.0
+ AHD (Random-Mask)	50.8 ↑0.8	22.5 ↑7.1	77.3 ↑0.2
+ AHD (Mask-One)	44.8 ↓5.2	13.9 ↓1.5	77.5 ↓0.4
+ AHD (Mask-Two)	43.0 ↓7.0	13.2 ↓2.2	77.5 ↓0.4
+ AHD (Mask-Three)	45.6 ↓4.4	13.9 ↓1.5	77.5 ↓0.4
+ AHD (Mask-Two) + Linear Probing [52]	42.8 ↓7.2	13.5 ↓1.9	77.1 ↑0.0
+ AID (AHD + RD)	41.8 ↓8.2	13.0 ↓2.4	77.1 ↑0.0

Table 5. **Ablation study for the designed components of AID.**

4.3. Ablation Studies

Impact of Masking Different Visual Areas. To evaluate the effect of masking Hijackers in various visual regions, we sequentially masked the Hijackers’ visual areas from top to bottom. The mask area was gradually increased to assess how AID’s performance would respond, using CHAIR as the benchmark and LLaVA-1.5-7B as the backbone model. As shown in Fig. 7, both CHAIR_I and CHAIR_s scores increased as the mask moved downward. When the entire visual area was masked, performance improved significantly above the baseline, indicating that removing all visual information effectively isolates the impact of the Hijackers. This suggests that in self-interacting image regions, the lower area accumulates more visual information, with tokens in this region exerting a greater influence on the Hijackers.

Effectiveness of Attention Hijacker Detection. To evaluate each component of AID, we conduct ablation studies on At-



LLaVA1.5 Default: The image depicts a train traveling through a tunnel, with **multiple cars attached to it...** There are several benches placed along the train tracks, providing seating for passengers waiting for the train. **The benches are positioned at various distances from the train...**

LLaVA1.5+VCD: The image depicts a train traveling through a tunnel, with **multiple tracks running alongside it...** There are several lights installed along the train **tracks**, illuminating the area for passengers. The lights are spaced at ...

LLaVA1.5+AID (Ours): The image depicts a train traveling through a tunnel, with **a green and white color scheme...** The train is positioned in the middle of the scene, with the tunnel **stretching out behind it**. The people are scattered throughout the image, with some standing closer to the train and others further away...

Figure 8. **Case Study.** AID effectively reduces hallucinations, outperforming VCD in visual scene understanding.

tention Hijackers Detection (AHD) and Re-Disentanglement (RD) using the CHAIR benchmark. As shown in Tab. 5, randomly masking instruction tokens (*Random-Mask*) increase CHAIR_s and CHAIR_I, likely due to unintentionally masking essential tokens, disrupting semantics, and increasing hallucinations. In contrast, AHD selectively masks Hijackers, reducing hallucinations by 5.2% and 1.5% on CHAIR_s and CHAIR_I, demonstrating its effectiveness. Additionally, masking two Hijackers (*Mask-Two*) yields optimal results, while masking three (*Mask-Three*) offers less improvement. Thus, we empirically set the masked Hijacker count to 2.

Effectiveness of Re-Disentanglement. To validate the effectiveness of Re-Disentanglement (RD) in addressing excessive masking, we compare it with the widely used Linear Probing approach [21, 40, 49, 52], which trains a linear model on hidden states to identify hallucinations while minimizing unnecessary operations. As shown in Tab. 5, *AHD+Linear Probing* offers minimal improvement over *AHD(Mask-Two)*, whereas *AHD+RD* reduces hallucinations by 8.2% and 2.4% on CHAIR_s and CHAIR_I, while maintaining recall. Unlike Linear Probing, RD requires no additional training, making it a more efficient solution.

4.4. Visualization Results

To evaluate AID’s effectiveness on image captioning, we compare it with LLaVA-1.5 and VCD. As shown in Fig. 8, LLaVA-1.5 generates hallucinated details, such as “multiple cars attached” and “benches positioned at various distances”. In contrast, our AID accurately describes visual details like “green and white color scheme” of the train and the peo-

ple’s positions relative to it, avoiding irrelevant information. This demonstrates that AID improves accuracy and reduces hallucinations, especially in complex scenes.

5. Conclusion

This paper presents a new perspective on hallucination mitigation, identifying it as interference from instruction tokens, or “Attention Hijacking”. We propose AID (Attention HIjackers Detection and Disentanglement), a training-free strategy that detects and disentangles these Hijackers to restore proper attention. A potential negative impact is that AID focuses on improving image understanding and does not address factual accuracy issues. Future work, by integrating RAG, could help mitigate this limitation.

References

- [1] Jean-Baptiste Alayrac, Jeff Donahue, Pauline Luc, Antoine Miech, Iain Barr, Yana Hasson, Karel Lenc, Arthur Mensch, Katherine Millican, Malcolm Reynolds, et al. Flamingo: a visual language model for few-shot learning. *Advances in Neural Information Processing Systems*, 35:23716–23736, 2022. 1
- [2] Dosovitskiy Alexey. An image is worth 16x16 words: Transformers for image recognition at scale. *arXiv preprint arXiv:2010.11929*, 2020. 3
- [3] Wenbin An, Feng Tian, Sicong Leng, Jiahao Nie, Haonan Lin, QianYing Wang, Guang Dai, Ping Chen, and Shijian Lu. Agla: Mitigating object hallucinations in large vision-language models with assembly of global and local attention. *arXiv preprint arXiv:2406.12718*, 2024. 2, 3
- [4] Jinze Bai, Shuai Bai, Shusheng Yang, Shijie Wang, Sinan Tan, Peng Wang, Junyang Lin, Chang Zhou, and Jingren Zhou. Qwen-vl: A versatile vision-language model for understanding, localization, text reading, and beyond. *arXiv preprint arXiv:2308.12966*, 2023. 6
- [5] Jinze Bai, Shuai Bai, Shusheng Yang, Shijie Wang, Sinan Tan, Peng Wang, Junyang Lin, Chang Zhou, and Jingren Zhou. Qwen-vl: A frontier large vision-language model with versatile abilities. *arXiv preprint arXiv:2308.12966*, 2023. 1
- [6] Ali Furkan Biten, Lluís Gómez, and Dimosthenis Karatzas. Let there be a clock on the beach: Reducing object hallucination in image captioning. In *Proceedings of the IEEE/CVF Winter Conference on Applications of Computer Vision*, pages 1381–1390, 2022. 2, 3
- [7] Beita Chen, Xinyu Lyu, Lianli Gao, Jingkuan Song, and Heng Tao Shen. Alleviating hallucinations in large vision-language models through hallucination-induced optimization. *arXiv preprint arXiv:2405.15356*, 2024. 2
- [8] Zhiyang Chen, Yousong Zhu, Yufei Zhan, Zhaowen Li, Chaoyang Zhao, Jinqiao Wang, and Ming Tang. Mitigating hallucination in visual language models with visual supervision. *arXiv preprint arXiv:2311.16479*, 2023. 4
- [9] Zhaorun Chen, Zhuokai Zhao, Hongyin Luo, Huaxiu Yao, Bo Li, and Jiawei Zhou. Halc: Object hallucination reduction via adaptive focal-contrast decoding. *arXiv preprint arXiv:2403.00425*, 2024. 6, 7
- [10] Yung-Sung Chuang, Yujia Xie, Hongyin Luo, Yoon Kim, James Glass, and Pengcheng He. Dola: Decoding by contrasting layers improves factuality in large language models. *arXiv preprint arXiv:2309.03883*, 2023. 6
- [11] Wenliang Dai, Junnan Li, Dongxu Li, Anthony Meng Huat Tiong, Junqi Zhao, Weisheng Wang, Boyang Li, Pascale Fung, and Steven Hoi. Instructclip: Towards general-purpose vision-language models with instruction tuning. *arXiv preprint arXiv:2306.04387*, 2023. 1
- [12] Timothée Darcet, Maxime Oquab, Julien Mairal, and Piotr Bojanowski. Vision transformers need registers. *arXiv preprint arXiv:2309.16588*, 2023. 3, 4
- [13] Alexey Dosovitskiy, Lucas Beyer, Alexander Kolesnikov, Dirk Weissenborn, Xiaohua Zhai, Thomas Unterthiner, Mostafa Dehghani, Matthias Minderer, Georg Heigold, Sylvain Gelly, Jakob Uszkoreit, and Neil Houlsby. An image is worth 16x16 words: Transformers for image recognition at scale. In *ICLR*, 2021. 2
- [14] Danny Driess, Fei Xia, Mehdi SM Sajjadi, Corey Lynch, Aakanksha Chowdhery, Brian Ichter, Ayzaan Wahid, Jonathan Tompson, Quan Vuong, Tianhe Yu, et al. Palm-e: An embodied multimodal language model. *arXiv preprint arXiv:2303.03378*, 2023. 1
- [15] Chaoyou Fu, Peixian Chen, Yunhang Shen, Yulei Qin, Mengdan Zhang, Xu Lin, Zhenyu Qiu, Wei Lin, Jinrui Yang, Xiawu Zheng, et al. Mme: A comprehensive evaluation benchmark for multimodal large language models. *arXiv preprint arXiv:2306.13394*, 2023. 6, 7
- [16] Team GLM, Aohan Zeng, Bin Xu, Bowen Wang, Chenhui Zhang, Da Yin, Diego Rojas, Guanyu Feng, Hanlin Zhao, Hanyu Lai, Hao Yu, Hongning Wang, Jiadai Sun, Jiajie Zhang, Jiale Cheng, Jiayi Gui, Jie Tang, Jing Zhang, Juanzi Li, Lei Zhao, Lindong Wu, Lucen Zhong, Mingdao Liu, Minlie Huang, Peng Zhang, Qinkai Zheng, Rui Lu, Shuaiqi Duan, Shudan Zhang, Shulin Cao, Shuxun Yang, Weng Lam Tam, Wenyi Zhao, Xiao Liu, Xiao Xia, Xiaohan Zhang, Xiaotao Gu, Xin Lv, Xinghan Liu, Xinyi Liu, Xinyue Yang, Xixuan Song, Xunkai Zhang, Yifan An, Yifan Xu, Yilin Niu, Yuantao Yang, Yueyan Li, Yushi Bai, Yuxiao Dong, Zehan Qi, Zhaoyu Wang, Zhen Yang, Zhengxiao Du, Zhenyu Hou, and Zihan Wang. Chatglm: A family of large language models from glm-130b to glm-4 all tools. *arXiv preprint arXiv:2406.12793*, 2024. 6
- [17] Xuan Gong, Tianshi Ming, Xinpeng Wang, and Zhihua Wei. Damro: Dive into the attention mechanism of lylv to reduce object hallucination. *arXiv preprint arXiv:2410.04514*, 2024. 2, 3, 4
- [18] Anisha Gunjal, Jihan Yin, and Erhan Bas. Detecting and preventing hallucinations in large vision language models. *arXiv preprint arXiv:2308.06394*, 2023. 1, 3
- [19] Qidong Huang, Xiaoyi Dong, Pan Zhang, Bin Wang, Conghui He, Jiaqi Wang, Dahu Lin, Weiming Zhang, and Nenghai Yu. Opera: Alleviating hallucination in multi-modal large language models via over-trust penalty and retrospection-allocation. *arXiv preprint arXiv:2311.17911*, 2023. 6
- [20] Fushuo Huo, Wenchao Xu, Zhong Zhang, Haozhao Wang, Zhicheng Chen, and Peilin Zhao. Self-introspective decoding:

Alleviating hallucinations for large vision-language models. *arXiv preprint arXiv:2408.02032*, 2024. 2, 3

[21] Che Jiang, Biqing Qi, Xiangyu Hong, Dayuan Fu, Yang Cheng, Fandong Meng, Mo Yu, Bowen Zhou, and Jie Zhou. On large language models' hallucination with regard to known facts. 2024. 8

[22] Jared Kaplan, Sam McCandlish, Tom Henighan, Tom B Brown, Benjamin Chess, Rewon Child, Scott Gray, Alec Radford, Jeffrey Wu, and Dario Amodei. Scaling laws for neural language models. *arXiv preprint arXiv:2001.08361*, 2020. 3

[23] Jae Myung Kim, A Koepke, Cordelia Schmid, and Zeynep Akata. Exposing and mitigating spurious correlations for cross-modal retrieval. In *Proceedings of the IEEE/CVF Conference on Computer Vision and Pattern Recognition*, pages 2584–2594, 2023. 3

[24] Sicong Leng, Hang Zhang, Guanzheng Chen, Xin Li, Shijian Lu, Chunyan Miao, and Lidong Bing. Mitigating object hallucinations in large vision-language models through visual contrastive decoding. *arXiv preprint arXiv:2311.16922*, 2023. 6

[25] Junnan Li, Dongxu Li, Silvio Savarese, and Steven Hoi. Blip-2: Bootstrapping language-image pre-training with frozen image encoders and large language models. *arXiv preprint arXiv:2301.12597*, 2023. 1

[26] Lei Li, Yuwei Yin, Shicheng Li, Liang Chen, Peiyi Wang, Shuhuai Ren, Mukai Li, Yazheng Yang, Jingjing Xu, Xu Sun, et al. A large-scale dataset towards multi-modal multilingual instruction tuning. *arXiv preprint arXiv:2306.04387*, 2023. 3

[27] Yifan Li, Yifan Du, Kun Zhou, Jinpeng Wang, Wayne Xin Zhao, and Ji-Rong Wen. Evaluating object hallucination in large vision-language models. *arXiv preprint arXiv:2305.10355*, 2023. 1, 2, 3, 6

[28] Tsung-Yi Lin, Michael Maire, Serge Belongie, James Hays, Pietro Perona, Deva Ramanan, Piotr Dollár, and C Lawrence Zitnick. Microsoft coco: Common objects in context. In *Computer Vision–ECCV 2014: 13th European Conference, Zurich, Switzerland, September 6–12, 2014, Proceedings, Part V 13*, pages 740–755. Springer, 2014. 6

[29] Fuxiao Liu, Kevin Lin, Linjie Li, Jianfeng Wang, Yaser Yacoob, and Lijuan Wang. Aligning large multi-modal model with robust instruction tuning. *arXiv preprint arXiv:2306.14565*, 2023. 3

[30] Fuxiao Liu, Kevin Lin, Linjie Li, Jianfeng Wang, Yaser Yacoob, and Lijuan Wang. Mitigating hallucination in large multi-modal models via robust instruction tuning. *arXiv preprint arXiv:2306.14565*, 2023. 1, 2

[31] Haotian Liu. Llava: Large language and vision assistant, 2024. <https://github.com/haotian-liu/LLaVA/tree/v1.2.2.7>

[32] Haotian Liu, Chunyan Li, Qingyang Wu, and Yong Jae Lee. Visual instruction tuning. *arXiv preprint arXiv:2304.08485*, 2023. 6

[33] Shi Liu, Kecheng Zheng, and Wei Chen. Paying more attention to image: A training-free method for alleviating hallucination in lylms. *arXiv preprint arXiv:2407.21771*, 2024. 2, 3

[34] Yuan Liu, Haodong Duan, Yuanhan Zhang, Bo Li, Songyang Zhang, Wangbo Zhao, Yike Yuan, Jiaqi Wang, Conghui He, Ziwei Liu, Kai Chen, and Dahu Lin. Mmbench: Is your multi-modal model an all-around player? *arXiv preprint arXiv:2307.06281*, 2023. 6

[35] Holy Lovenia, Wenliang Dai, Samuel Cahyawijaya, Ziwei Ji, and Pascale Fung. Negative object presence evaluation (nope) to measure object hallucination in vision-language models. *arXiv preprint arXiv:2310.05338*, 2023. 1, 3

[36] OpenAI. GPT-4V(ision) system card. 2023. 1

[37] Hadas Orgad, Michael Toker, Zorik Gekhman, Roi Reichart, Idan Szpektor, Hadas Kotek, and Yonatan Belinkov. Llms know more than they show: On the intrinsic representation of llm hallucinations. *arXiv preprint arXiv:2410.02707*, 2024. 2

[38] Reiner Pope, Sholto Douglas, Aakanksha Chowdhery, Jacob Devlin, James Bradbury, Jonathan Heek, Kefan Xiao, Shivanai Agrawal, and Jeff Dean. Efficiently scaling transformer inference. 2023. 3

[39] Anna Rohrbach, Lisa Anne Hendricks, Kaylee Burns, Trevor Darrell, and Kate Saenko. Object hallucination in image captioning. *arXiv preprint arXiv:1809.02156*, 2018. 2, 3, 6

[40] Weihang Su, Changyue Wang, Qingyao Ai, Yiran Hu, Zhijing Wu, Yujia Zhou, and Yiqun Liu. Unsupervised real-time hallucination detection based on the internal states of large language models. 2024. 8

[41] Zhiqing Sun, Sheng Shen, Shengcao Cao, Haotian Liu, Chunyuan Li, Yikang Shen, Chuang Gan, Liang-Yan Gui, Yu-Xiong Wang, Yiming Yang, et al. Aligning large multi-modal models with factually augmented rlhf. *arXiv preprint arXiv:2309.14525*, 2023. 2, 3

[42] Junyang Wang, Yiyang Zhou, Guohai Xu, Pengcheng Shi, Chenlin Zhao, Haiyang Xu, Qinghao Ye, Ming Yan, Ji Zhang, Jihua Zhu, et al. Evaluation and analysis of hallucination in large vision-language models. *arXiv preprint arXiv:2308.15126*, 2023. 3

[43] Weihan Wang, Qingsong Lv, Wenmeng Yu, Wenyi Hong, Ji Qi, Yan Wang, Junhui Ji, Zhuoyi Yang, Lei Zhao, Xixuan Song, et al. CogVLM: Visual expert for pretrained language models. *arXiv preprint arXiv:2311.03079*, 2023. 1

[44] Jason Wei, Yi Tay, Rishi Bommasani, Colin Raffel, Barret Zoph, Sebastian Borgeaud, Dani Yogatama, Maarten Bosma, Denny Zhou, Donald Metzler, et al. Emergent abilities of large language models. *arXiv preprint arXiv:2206.07682*, 2022. 3

[45] Thomas Wolf, Lysandre Debut, Victor Sanh, Julien Chau- mond, Clement Delangue, Anthony Moi, Pierrick Cistac, Tim Rault, Rémi Louf, Morgan Funtowicz, Joe Davison, Sam Shleifer, Patrick von Platen, Clara Ma, Yacine Jernite, Julien Plu, Canwen Xu, Teven Le Scao, Sylvain Gugger, Mariama Drame, Quentin Lhoest, and Alexander M. Rush. Huggingface's transformers: State-of-the-art natural language processing. *ArXiv*, abs/1910.03771, 2019. 6

[46] Yun Xing, Yiheng Li, Ivan Laptev, and Shijian Lu. Mitigating object hallucination via concentric causal attention. *arXiv preprint arXiv:2410.15926*, 2024. 2, 3

[47] Qinghao Ye, Haiyang Xu, Guohai Xu, Jiabo Ye, Ming Yan, Yiyang Zhou, Junyang Wang, Anwen Hu, Pengcheng Shi,

Yaya Shi, Chenliang Li, Yuanhong Xu, Hehong Chen, Jun-feng Tian, Qian Qi, Ji Zhang, and Fei Huang. mplug-owl: Modularization empowers large language models with multi-modality. *arXiv preprint arXiv:2304.14178*, 2023. 6

[48] Tianyu Yu, Yuan Yao, Haoye Zhang, Taiwen He, Yifeng Han, Ganqu Cui, Jinyi Hu, Zhiyuan Liu, Hai-Tao Zheng, Maosong Sun, et al. Rhf-v: Towards trustworthy mllms via behavior alignment from fine-grained correctional human feedback. *arXiv preprint arXiv:2312.00849*, 2023. 2

[49] Tian Yu, Shaolei Zhang, and Yang Feng. Truth-aware context selection: Mitigating the hallucinations of large language models being misled by untruthful contexts. *arXiv preprint arXiv:2403.07556*, 2024. 8

[50] Weihao Yu, Zhengyuan Yang, Linjie Li, Jianfeng Wang, Kevin Lin, Zicheng Liu, Xinchao Wang, and Lijuan Wang. Mm-vet: Evaluating large multimodal models for integrated capabilities. In *Forty-first International Conference on Machine Learning*, 2024. 6

[51] Yan Zeng, Xinsong Zhang, and Hang Li. Multi-grained vision language pre-training: Aligning texts with visual concepts. *arXiv preprint arXiv:2111.08276*, 2021. 3

[52] Qinyu Zhao, Ming Xu, Kartik Gupta, Akshay Asthana, Liang Zheng, and Stephen Gould. The first to know: How token distributions reveal hidden knowledge in large vision-language models? *arXiv preprint arXiv:2403.09037*, 2024. 4, 8

[53] Zhiyuan Zhao, Bin Wang, Linke Ouyang, Xiaoyi Dong, Jiaqi Wang, and Conghui He. Beyond hallucinations: Enhancing lvlms through hallucination-aware direct preference optimization. *arXiv preprint arXiv:2311.16839*, 2023. 2

[54] Yiyang Zhou, Chenhang Cui, Jaehong Yoon, Linjun Zhang, Zhun Deng, Chelsea Finn, Mohit Bansal, and Huaxiu Yao. Analyzing and mitigating object hallucination in large vision-language models. *arXiv preprint arXiv:2310.00754*, 2023. 3

[55] Deyao Zhu, Jun Chen, Xiaoqian Shen, Xiang Li, and Mohamed Elhoseiny. Minigpt-4: Enhancing vision-language understanding with advanced large language models. *arXiv preprint arXiv:2304.10592*, 2023. 1

[56] Deyao Zhu, Jun Chen, Xiaoqian Shen, Xiang Li, and Mohamed Elhoseiny. Minigpt-4: Enhancing vision-language understanding with advanced large language models. *arXiv preprint arXiv:2304.10592*, 2023. 6

[57] Xianwei Zhuang, Zhihong Zhu, Yuxin Xie, Liming Liang, and Yuexian Zou. Vasparsc: Towards efficient visual hallucination mitigation for large vision-language model via visual-aware sparsification. *arXiv preprint arXiv:2501.06553*, 2025. 7